Electronic Preprint for Journal of Information Processing Vol.29

Regular Paper

# Maneuver and Turn Classification in Wheelchair Basketball Using Inertial Sensors

Ryosuke Hasegawa[1,a)] Akira Uchiyama[1,b)] Takuya Magome[2,c)] Juri Tatsumi[2,d)]
Teruo Higashino[1,e)]

Received: April 6, 2020, Accepted: October 6, 2020

**Abstract:** In wheelchair basketball (WB), players are constantly trying to improve their wheelchair maneuvering techniques since these are the most basic and important actions in all situations. However, assessing maneuvering quality is difficult due to the lack of quantitative metrics. In this paper, we propose two classification methods for maneuvering actions and turns by focusing on the specific wheelchair movement. For this purpose, inertial sensors are fixed to the left and right wheels of the wheelchair. In maneuver classification, the occurrence of maneuvers is detected using the angular velocity. Major maneuver activities in WB are classified into 2 types: *PUSH* and *PULL*. First, our method segments candidates of maneuver periods by the local maximum/minimum of the angular velocity since the rotation of the wheel generated by maneuvering that leads to sharp changes in the angular velocity. We then classify maneuvering actions based on thresholds. As for the turn classification, we first detect turns by calculating the amount of wheelchair rotation from the angular velocities of both wheels. We then classify the detected turns into *PIVOT* and *TURN* by using thresholds based on the typical movement of both wheels during each turn. To evaluate the performance of the proposed maneuver classification method, we collected real data from 6 players. From the result, we confirmed our method achieves an average recall and precision of 91.9% and 84.6% for maneuver classification, respectively. The results also show that our turn classification achieves an average recall and precision of 99.7% and 99.7%, respectively. Furthermore, we confirmed the effectiveness of the classification results for the assessment of maneuver quality.

**Keywords:** wheelchair basketball, sports data analysis, activity recognition

## 1. Introduction

Emerging developments in sensing technology have focused the attention of athletes, coaches and fans on applying it to data analysis in sports training, strategies and entertainment [1]. One of major challenges in sports data analysis is to design sophisticated methods suitable for target sports for useful data collection. In major sports such as football, basketball, and baseball, data analysis is already essential since many engineers and researchers have developed practical systems to apply it. However, data analysis in wheelchair basketball (WB) still requires further effort to establish building blocks essential for data analysis.

Therefore, we have been working on the development of a system to support WB data analysis in cooperation with athletes and coaches. In WB, players constantly strive to improve their wheelchair movement techniques since it is important to be able to move the wheelchair quickly and efficiently depending on the time and position. In particular, the wheelchair maneuvering, which is movement of the wheel, is the most basic and important action in all situations. However, the assessment of maneuvering quality is difficult due to the lack of quantitative metrics. To support quantitative analysis of the maneuver quality in this paper, we propose a method to detect and classify maneuver actions using inertial sensors. We define the target maneuver actions as *PUSH* and *PULL* through discussion with experts because statistics such as strength and interval of these actions are closely related to the quality of the maneuver. *PUSH* is the maneuver of grabbing the rim and pushing it forward to accelerate the wheel, while *PULL* is the maneuver of grabbing the rim and stopping the wheel or pulling it backwards to decelerate it. Although camera-based approaches are widely used for sports data analysis, they cannot measure such precise motions. To deal with this problem we first of all clamped two inertial sensors to the left and right wheels of the wheelchair to measure the angular velocity of each wheel. Even using inertial sensors, the classification of maneuver actions is still challenging because of various movements of wheels with different speeds and directions. To clarify the maneuvering actions concealed within such complicated movements we employ a segmentation algorithm followed by classification. First, we segment candidates of maneuver periods by the local maximum/minimum of the angular velocity since the rotation of the wheel generated by maneuvering leads to sharp changes in the angular velocity. Then, we classify maneuver actions in each segment based on thresholds.

In addition to the maneuver, wheelchair behavior is also impor-

1 Graduate School of Information Science and Technology, Osaka University, Suita, Osaka 565–0871, Japan
2 Otemon Gakuin University, Ibaraki, Osaka 567–8502, Japan
a) r-hasegawa@ist.osaka-u.ac.jp
b) uchiyama@ist.osaka-u.ac.jp
c) t-magome@otemon.ac.jp
d) Juri.Tatsumi.34@otemon.ac.jp
e) higashino@ist.osaka-u.ac.jp

tant. In this paper, we design a method to classify types of turns into *PIVOT* and *TURN*. This is because the pivot turn is one of the most important techniques in WB to push an opponent away by applying power efficiently. For this purpose, similarly to the maneuver classification, we detect any turns by calculating the amount of wheelchair rotation from the angular velocities of the both wheels. We then identify *PIVOT* turns based on thresholds for each wheel based on the typical movement of the pivot turns.

In order to evaluate the performance of the proposed maneuver classification method, we collected data from six players in a WB practice game containing 1,005 *PUSH* and 152 *PULL* actions. From the results, we confirmed that the precision and recall of both maneuver classifications are more than 84.6%. We also collected data from 172 pivots and 192 turns to evaluate our turn classification. The result shows our method successfully classifies *PIVOT* and *TURN* with an F-measure of 99.7%. Furthermore, we show the effectiveness of our classification results in assessing maneuver quality through maneuver analysis combined with other information such as player positions.

Our contributions are summarized as follows.

- We developed a system to support the data analysis in wheelchair basketball by using inertial sensors and a camera.
- We designed methods to classify maneuver actions and turns in wheelchair basketball by focusing on specific movement of wheels.
- We evaluated the performance of our methods by collecting data from athletes.
- We showed the potential of the classification results through the analysis of data collected in a practice game.

## 2. Related Work

There have been several studies on WB. For example, Refs. [2], [3], [4] study the relationship between the level of disabilities and the performance. This relationship must be determined in order to harmonize players with different level of disabilities, so a classification system is used to evaluate the functional abilities of players on a point scale of 1 to 4.5. Reference [2] reports the level of disability and the number of successful shots and passes are correlated for professional female WB players. These studies do not investigate the design of data analysis in WB because they focus on the medical aspect of WB rather than sports. Also, other studies from a medical perspective investigate the risk of heatstroke [5] or injury [6] during training and games.

Some research work on quantifying athletic performance is carried out by investigating the relationship between moving speeds and wheelchair configurations [7], [8], [9]. Such studies reveal the effectiveness of data analysis in WB although they rely on the measured raw data of acceleration and angular velocity in controlled environment. However, it is important for players and coaches to collect useful data related to performance in uncontrolled environment (i.e., games and training). Therefore, our goal is to extract meaningful data from WB players in actual situations. Towards this goal, we focus on the detection and classification of maneuver actions and turns as the building blocks of WB data analysis.

## 3. System Overview

**Figure 1** illustrates an overview of our system. Instead of manual video analysis currently used by many teams, we extract statistics from videos and inertial sensors. **Figure 2** shows a snapshot of our system developed for players and coaches. Our system provides player tracking and visualization of statistics on wheelchair movement. For player tracking, we have implemented DeePSORT [10], [11] combined with YOLOv3 [12] for object detection. Since YOLOv3 itself cannot detect wheelchairs, we trained the model by using 602 images of wheelchairs cropped from videos of WB.

On the other hand, precise motions such as maneuver of wheelchairs are extracted from inertial sensors. In this paper, we aim at designing a method to detect and classify *PUSH* and *PULL* actions of wheelchair maneuvering. We also design a method to detect and classify *PIVOT* and *TURN*. This leads to the quantification of the maneuver quality by analyzing statistics related to the detected actions. Furthermore, the detection results can be used for the analysis of strategies and performance assessment in combination with other information such as players positions. In WB, the basic strategy is to screen and block the defending opponent and help a team member with making shots. This is very effective because a wheelchair needs a large area to turn. Therefore, it is important to analyze how the wheelchair is manipulated to move to the proper position to allow shooting and blocking. **Figure 3** illustrates an example situation in which a pivot turn is more efficient than a spin turn. When the position in front of a player is blocked by an opponent, a pivot turn is more efficient for

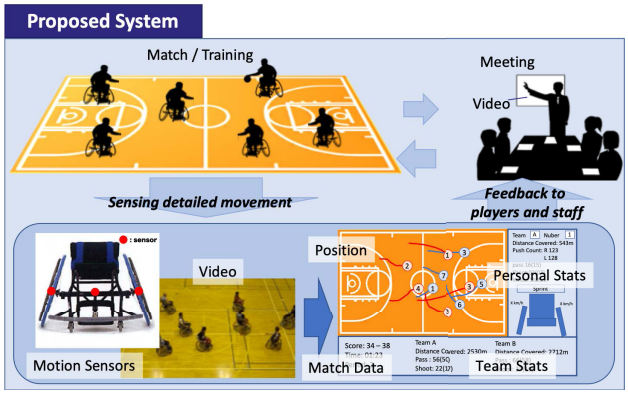


**Fig. 1** System overview.

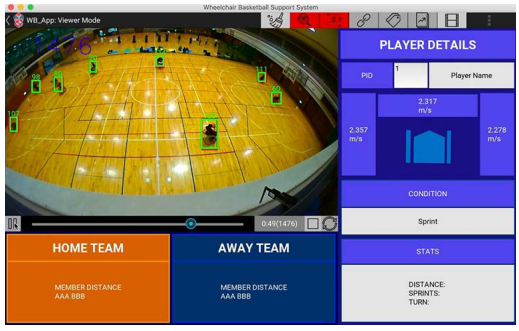


**Fig. 2** Snapshot of support system.

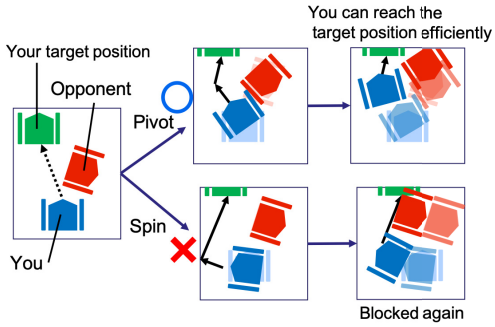


**Fig. 3** Effectiveness of pivot turn.

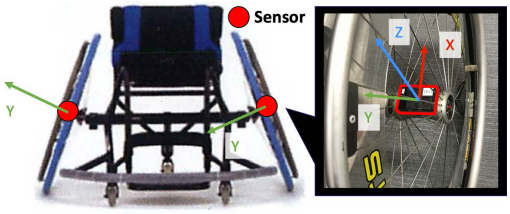


**Fig. 4** Sensor equipment.

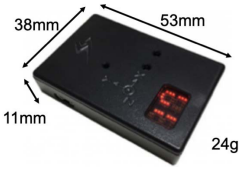


**Fig. 5** 9-axis motion sensor.

**Table 1** Sensor measurement range.

| Sensor | Unit | Range |
|---|---|---|
| Acceleration | G | [−16, +16] |
| Angular Velocity | dps | [−1500, +1500] |
| Magnetic Field | Gauss | [−10, +10] |

moving forward because the player can move along a straighter path toward the target position by changing the direction of the opponent. If the player changes direction without a pivot turn, the opponent can easily screen that player by moving back and forth.

As shown in **Fig. 4**, inertial sensors are fixed to the axles of the left and right wheels. We use DSP wireless 9-axis motion sensors manufactured by SPORTS SENSING Co., LTD [*1] (**Fig. 5**). The sensor is capable of measuring 3-axis acceleration, 3-axis angular velocity, and 3-axis geomagnetic data at a sampling rate of 200 Hz. The measurement ranges of the sensor are shown in **Table 1**. Hereafter, we use [*radians*/*second*] as the unit of angular velocity unless otherwise stated.

## 4. Maneuver Classification

### 4.1 Overview

The overview of the proposed method is illustrated in **Fig. 6**. The maneuver actions in WB are instantaneous movements consisting of independent movements of left and right wheels. This means we need an approach different from activity recognition for continuous motions such as walking. Therefore, our method firstly segments the time series of the angular velocity to extract

[*1] https://www.sports-sensing.com/products/sensor/dspmotion/dspms.html


**Fig. 6** Method overview.

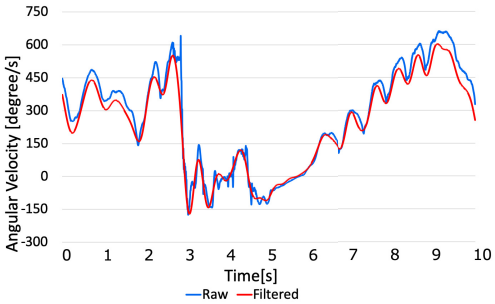


**Fig. 7** Example of filtered angular velocity.

candidate periods of *PUSH* and *PULL* motions without any fixed window size. We then classify the maneuver actions for each segment. Our target actions are *PUSH* and *PULL* since they are frequently observed in WB. *PUSH* is the motion to apply force the wheel to the forward direction while the *PULL* is the motion to apply force in the reverse (backward) direction. Since the segmented periods are still the candidates of *PUSH* and *PULL*, there is a possibility of other actions. We define the other actions as *OTHERS* and design a classification method for the three maneuver actions. The classification is performed by thresholds for the angular velocity. Finally, we remove the segment classified *PULL* when wheelchairs collide with each other because the change in angular velocity is greatly affected by collision rather than *PULL*.

### 4.2 Preprocessing

Since the raw sensor data contains noise, we apply a Chebyshev type I filter [13] which is a low pass filter using the Chebyshev polynomials. The Chebyshev polynomials of the first kind are defined by the recurrence relation.

$$T_0(x) = 1 \tag{1}$$

$$T_1(x) = x \tag{2}$$

$$T_{n+1}(x) = 2xT_n(x) - T_{n-1}(x) \tag{3}$$

The ordinary generating function for $T_n$ is

$$\sum_{n=0}^{\infty} T_n(x)t^n = \frac{1 - tx}{1 - 2tx + t^2} \tag{4}$$

We let $G_n(\Omega)$ be a function of the angular frequency $\Omega$ of the $n$-th order low-pass filter as below.

$$G_n(\Omega) = \frac{1}{\sqrt{1 + \varepsilon^2 T_n^2\left(\dfrac{\Omega}{\Omega_0}\right)}} \tag{5}$$

Where $\varepsilon$, $\Omega_0$, and $T_n$ are a ripple factor, a cutoff frequency, and a Chebyshev polynomial of the $n$-th order, respectively. We empirically set the above parameters as $\varepsilon = 1.0$, $\Omega_0 = 0.03$, and $n = 6$. **Figure 7** illustrates an example of the filtering. We see that the raw data is smoothed by filtering the noise.

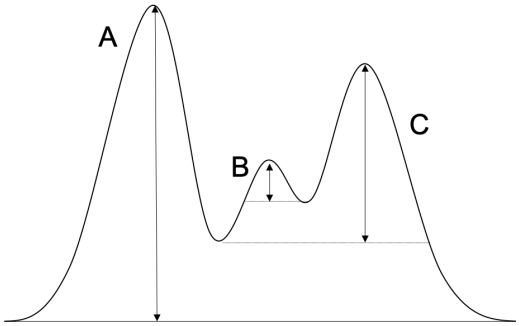


**Fig. 8** Example of prominence.

### 4.3 Segmentation

Each maneuver action consists of grip, move, and release. The time from the grip to the release widely varies even for the same action, which means that a sliding window with a fixed size does not work well. Therefore, we apply peak/valley detection in order to extract candidate segments of the maneuver actions from the time series of the angular velocity. We remove small peaks/valleys due to noise in addition to peaks/valleys detected within an extremely short interval.

The peak detection is performed as follows. We denote the angular velocity at time $t$ as $\omega(t)$. We then determine the time $t$ that satisfies the following condition (6) of a local maximum (peak).

$$\omega(t-1) < \omega(t) > \omega(t+1) \tag{6}$$

Similarly, we also find the time $t$ that satisfies the condition (7) of a local minimum (valley).

$$\omega(t-1) > \omega(t) < \omega(t+1) \tag{7}$$

To remove the peaks and valleys due to noise, we further apply noise filtering based on a prominence [14]. The prominence is used in signal processing to measure how much the peak is prominent considering the relative height to its surrounding peaks. An example of prominence is shown in **Fig. 8**. Vertical arrows show the prominence of three peaks on a prominence island which is the reference level of the prominence illustrated by the dashed horizontal lines in Fig. 8. The prominence island is defined as follows. First, we extend a horizontal line from a peak to the left and right until the line crosses the signal due to a higher peak or the end of the signal. Then, we find the minimum of the signal in each of the two intervals. Finally, the higher of the two intervals minimal specifies the reference level. The height of the peak above the reference level is its prominence. We analyzed the characteristics of the prominence of angular velocity peaks. **Figure 9** shows the prominence during practice and **Fig. 10** shows the height distribution of the prominence. We found there are many peaks with low prominence due to noise. We therefore chose to exclude peaks with a prominence of less than 20. If there are multiple peaks/valleys within $T_{min}$, all peaks/valleys except for the one with the largest/smallest value have also been removed since such extremely fast actions are impossible. **Table 2** shows the minimum interval between *PUSH* and *PULL* for six players during the game. From this result, the threshold of the minimum interval $T_{min}$ was set to 0.3.

Finally, we segment the time series of the angular velocity by

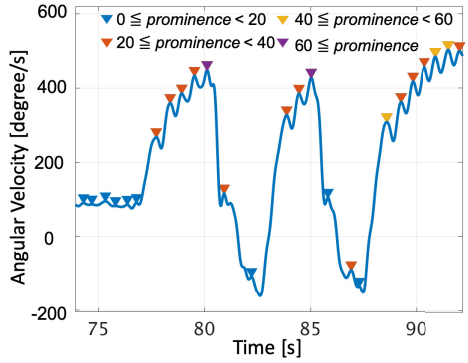


**Fig. 9** Prominence of angular velocity peaks during practice.

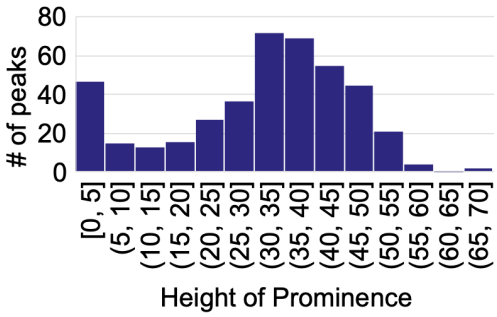


**Fig. 10** Distribution of the prominence.

**Table 2** Minimum maneuver interval [$s$] of players.

| | *PUSH* | | *PULL* | |
|---|---|---|---|---|
| Player ID | # of *PULL* | Min. Interval | # of*PULL* | Min. Interval |
| 1 | 113 | 0.33 | 40 | 1.13 |
| 2 | 72 | 0.30 | 31 | 0.86 |
| 3 | 63 | 0.33 | 35 | 0.90 |
| 4 | 90 | 0.33 | 32 | 1.53 |
| 5 | 105 | 0.30 | 36 | 1.00 |
| 6 | 80 | 0.40 | 38 | 1.06 |

the detected peaks and valleys. We let $d^i$ denote the $i$-th detected peak or valley for the time series of the detected peaks and valleys. Then, the $i$-th segment $s^i$ ($i > 0$) is defined as $(t(d^{i-1}), t(d^i)]$ where $t(d^i)$ is the time when $d^i$ is observed. Since there is no zero-th peak or valley, $t(d^0)$ is defined as 0 which is the start of the measurement.

### 4.4 Classification

We classify each segment into *PUSH*, *PUSH*, or *OTHERS*. However, the waveform greatly differs depending on the speed of the wheelchair even for the same *PUSH* actions. For example, **Fig. 11** shows the waveform of the angular velocity during a sprint. The first *PUSH* segment and the following *PUSH* segments are clearly different. A large velocity change occurs at the first *PUSH* while the velocity change in the following *PUSH* is not as large as the change in the first *PUSH*. This is due to the player's own ability and the speed just before *PUSH*.

The classification is performed as follows based on the above observation. Each segment $s^i$ is classified into *PUSH* if the following three conditions (8), (10), and (11) are satisfied. The *PUSH* action maximizes the speed in the short term. Therefore, the first condition is that $s^i$ ends at a peak. This is expressed as.

$$\omega(t(d^i)-1) < \omega(t(d^i)) > \omega(t(d^i)+1) \tag{8}$$

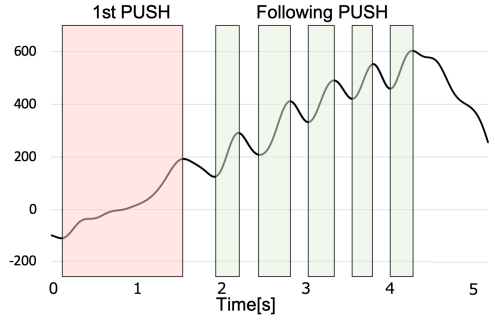


**Fig. 11** Example of *PUSH* angular velocity.

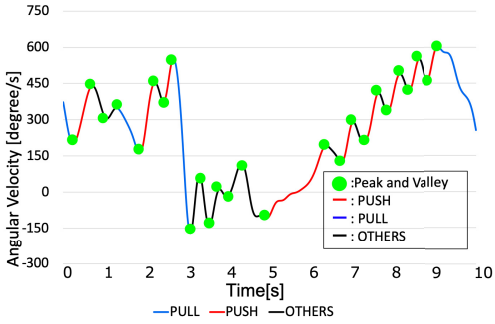


**Fig. 12** Example of classification result.

The second condition is that there is a large speed change within the segment period. Since the degree of the speed change depends on the player's ability, we determine the threshold $T_{\text{height}}$ for the amount of speed change considering the player's ability and the speed before the action. We consider the player's ability as the highest speed in a game or practice. When the maximum speed is $\omega_{max}$ and the angular velocity at the end of the previous segment is $\omega(t(d^{i-1}))$, the threshold $T_{\text{height}}$ of the speed change is defined as given below.

$$T_{\text{height}} = \begin{cases} \omega_{max}/16 & (\omega(t(d^{i-1})) >= \omega_{max}/4) \\ (\omega_{max} - 3\omega(t(d^{i-1})))/4 & (\omega_{max}/4 > \omega(t(d^{i-1})) > 0) \\ \omega_{max}/4 & (0 >= \omega(t(d^{i-1}))) \end{cases} \tag{9}$$

Since the amount of speed change within the segment periods must exceed this threshold, the second condition is given below.

$$\left| \max_{t\in(t(d^{i-1}),t(d^i))} \omega(t) - \min_{t\in(t(d^{i-1}),t(d^i))} \omega(t) \right| \geq T_{\text{height}} \tag{10}$$

The third condition is the rapid speed increase. The increase in speed occurs due to not only *PUSH* but also weight shifting and movement of the opposite wheel. On the other hand, in a *PUSH* action, it is necessary to grab the rim, leading to a slight instantaneous decrease in speed, before the speed increase. This leads to a significantly rapid increase of the angular velocity. Therefore, by using the threshold for the rapid speed increase $T_\delta^{PUSH}$, the third condition is represented as follows:

$$\max_{t\in(t(d^{i-1}),t(d^i))} \omega'(t) \geq T_\delta^{PUSH}, \tag{11}$$

where $\omega'(t)$ is the time derivative of $\omega(t)$. When the above three conditions (8), (10), and (11) are satisfied, segment $s^i$ is classified into *PUSH*.

On the other hand, each segment $s^i$ is classified into *PULL* if conditions (10), (12), and (14) are satisfied. Contrary to the *PUSH* action, the *PULL* action minimizes the speed in the short term. Therefore, the first condition is that $s^i$ ends at a valley. This is expressed as below.

$$\omega(t(d^i) - 1) > \omega(t(d^i)) < \omega(t(d^i) + 1) \tag{12}$$

The second condition is that there is a large speed change within the segment period. This is same as the condition (10) in *PUSH*. However, the threshold $T_{\text{height}}$ of the speed change is defined as given below.

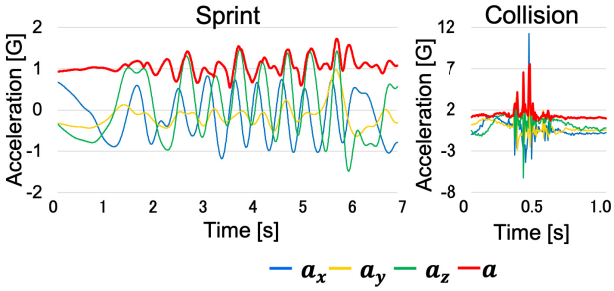


**Fig. 13** Example of acceleration during sprint and collision.

$$T_{\text{height}} = \begin{cases} \omega(t(d^{i-1})) - \omega_{max}/4 & (\omega(t(d^{i-1})) > \omega_{max}/2) \\ \omega_{max}/4 & (\omega_{max}/2 >= \omega(t(d^{i-1}))) \end{cases} \tag{13}$$

The third condition is the rapid speed decrease occurs. The decrease in speed occurs due to not only *PULL* but also to friction and weight shifting. On the other hand, a *PULL* action needs to grab the rim, resulting in a rapid decrease in speed. Therefore, by using the threshold for the rapid speed decrease $T_\delta^{PULL}$, the third condition is represented as follows.

$$\min_{t\in(t(d^{i-1}),t(d^i))} \omega'(t) \geq -T_\delta^{PULL} \tag{14}$$

Finally, all of the other segments are classified as *OTHERS*. An example of the classification result using the proposed method is shown in **Fig. 12**.

### 4.5 Remove Noise by Collision

Wheelchair collisions frequently occur during games. At that moment, a maneuver to stabilize the wheelchair may be performed. However, the wheel angular velocity decreases rapidly regardless of the occurrence of maneuvers. Such rapid decreases of the angular velocity are wrongly classified as *PULL*. To solve this problem, we detect collisions and change *PULL* labels within a fixed period from the collisions to *OTHERS*. We use acceleration to detect collisions. We also determined the threshold for collision detection and the duration of the period causing wrong *PULL* labels based on the statistics as follows.

The magnitude of 3 axis acceleration $a[G]$ can be expressed by the following equation.

$$a = \sqrt{a_x^2 + a_y^2 + a_z^2}\,[\text{G}] \tag{15}$$

The waveforms of the acceleration in sprint and collision are shown in **Fig. 13**. We see that the acceleration is obviously higher

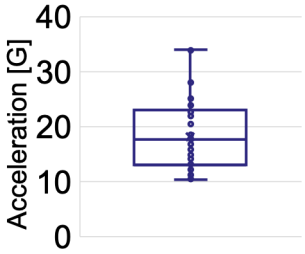


**Fig. 14** Distribution of maximum acceleration at collisions.

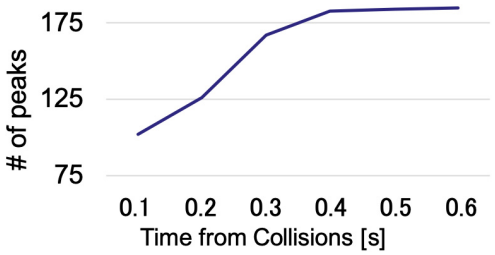


**Fig. 15** Number of peaks around collisions.

during the collision than the other cases. **Figure 14** shows the range of the maximum acceleration for 24 collisions observed during one minute of the preliminary experiment. The minimum value of the maximum acceleration was 10.17. Therefore, we detect a collision when $a$ exceeds 10 $[G]$. Figure 13 shows there are several peaks in addition to the maximum peak at collisions. In order to investigate the effect of the vibration caused by the collisions, the number of peaks that exceed 5 $[G]$, which is half of the acceleration threshold of 10, is analyzed within 0.1 to 0.6 seconds from the maximum peaks. As shown in **Fig. 15**, the number of peaks around the maximum peak increases as the range of time is expanded. We also found the increase is small around 0.5 seconds. Therefore, we determined the duration of the period causing wrong *PULL* labels as 0.5 seconds.

We note that the speed of the wheelchair does not increase upon collision. This means that collisions do not cause wrong *PUSH* labeling. Therefore, *PUSH* actions are not filtered since *PUSH* soon after the collisions typically shows a significant increase in the angular velocity which is totally different from wrong *PULL* labels due to collisions.

## 5. Turn Classification

### 5.1 Detection

We also classify turns of wheelchairs into *PIVOT* and *TURN* (the other turns). As **Fig. 16** shows, *PIVOT* is a change of direction with one fixed wheel while *TURN* is any other change in direction. *TURN* has two types of motions, curve and spin. A curve is an action where both wheels move in the same direction when changing the direction of the wheelchair, while spin moves the wheels in the opposite directions. From observations and discussions with players and coaches, we define turns as the movement with the rotation of wheelchairs of more than 60 degrees within 1.5 seconds.

To extract periods that meet the above definition, we calculate the rotation degree of the wheelchair based on the model of the two-differential wheeled robot [15]. From the inertial sensors, the

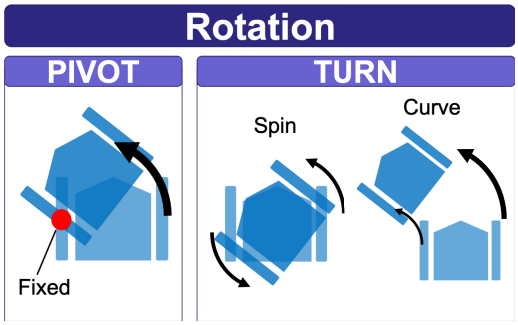


**Fig. 16** Type of rotation.

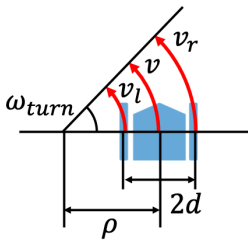


**Fig. 17** Wheelchair in turn.

angular velocities $\omega_{right} and \omega_{left}$ around the axles of the left and right wheels are obtained. Let $r$ denote the length of the radius of the wheel. The speeds of the left and right wheels $v_{right}$ and $v_{left}$ are then respectively expressed as below.

$$v_{right} = r * \omega_{right} \tag{16}$$
$$v_{left} = r * \omega_{left} \tag{17}$$

Next, we assume that the wheelchair is making a motion around the center of the rotation. As shown in **Fig. 17**, if the angular speed of turning is $\omega_{turn}$ and the radius of the turn is $\rho$, the speed at the center of the wheelchair $v$ is represented as shown below.

$$v = \rho\omega_{turn} \tag{18}$$

On the other hand, if the distance from the center to the wheel is $d$, the turn radii of each wheel increase or decrease by $d$, and the speeds of the left and right wheels are as follows.

$$v_{right} = (\rho + d)\omega_{turn} \tag{19}$$
$$v_{left} = (\rho - d)\omega_{turn} \tag{20}$$

Solving for the above formulas yields the following formula:

$$\omega_{turn} = (v_{right} - v_{left})/2d \tag{21}$$
$$v = (v_{right} + v_{left})/2 \tag{22}$$
$$\rho = d(v_{right} + v_{left})/(v_{right} - v_{left}), \tag{23}$$

where $\omega_{turn}$, $v$ and $\rho$ denote the rotation speed, forward speed and radius of rotation of the wheelchair, respectively. We use $\omega_{turn}$ to detect turns as we defined. The center of the rotation is on the left side of the direction of movement when $\rho$ is positive, and vice versa.

### 5.2 Classification

Next, for each detected turn, we classify whether it is a pivot

or not. During a pivot, one of the wheels is stationary. However, it is difficult to completely stop the wheel. We therefore use the amount of rotation of the wheel with lower speed during the turn. We represent the amount of rotation of the wheel with lower speed during the $i$-th turn as $\theta^i_{lower}$ defined as:

$$\theta^i_{lower} = \min\left[\sum_{t\in turn^i} \omega_{right}(t), \sum_{t\in turn^i} \omega_{left}(t)\right], \quad (24)$$

where $turn^i$ denotes the period of the $i$-th turn. If $\theta^i_{lower}$ is less than $\pi/4$, it is classified as *PIVOT*. In addition, if $\theta^i_{lower}$ exceeds $\pi/4$, the $i$-th turn is classified as *TURN*.

# 6. Evaluation

## 6.1 Maneuver Classification

### 6.1.1 Settings

We collected real data in a practice game for evaluation. The game duration was 317 seconds. We attached inertial sensors to wheelchairs of six players. The maximum speed observed by each player during the game is listed in the **Table 3**. We manually labeled the maneuver actions by recording a video. However, due to occlusion and image quality, the labeling was sometimes difficult. To deal with such ambiguity in manual labeling, we established the criteria of ground truth. We judged that the wheel was pushed when it was obvious that the player gripped the rim with the movement going forward based on the player's arm motion. We also identified *PULL* when it was obvious that the wheel suddenly decelerated or moving backward while the player gripped the rim based on the player's arm motion.

After labeling, a total of 1,157 maneuver actions were performed, consisting of 1,005 *PUSH* and 152 *PULL*. Since the ground-truth is labeled manually, we allow 1.5 seconds difference for the detection time or in other words the detected class is regarded as correct if the same ground-truth label exists within 1.5 seconds.

### 6.1.2 Results

#### 6.1.2.1 Threshold Configuration

In our method, we need to configure the thresholds appropriately. To see the difference in the thresholds for different players, we conducted a leave-one-person-out cross validation. The thresholds $T^{PUSH}_\delta$ and $T^{PULL}_\delta$ are set from 1.0 to 3.5 with increments of 0.25 as below.

$$(T^{PUSH}_\delta, T^{PULL}_\delta) \in [(1.0, 1.0), (1.0, 1.25), \ldots (3.5, 3.5)] \quad (25)$$

From the result shown in **Table 4**, we confirm the optimal threshold setting is the same among 5 of the 6 cases in the cross validation. However, we found that the F-measure of the player 3 is slightly worse than the others. This is mainly because the wheel size of the player 3 was larger than the others due to the wheelchair configuration. Therefore, we may adjust the thresholds according to the wheelchair configuration to improve the performance. In the following evaluation, the thresholds are set as $T^{PUSH}_\delta = 1.5$ and $T^{PULL}_\delta = 1.5$.

**Table 3** Max speed [degree/s] of players.

| Player ID | Max Speed (Left) | Max Speed (Right) |
|---|---|---|
| 1 | 675.7 | 667.8 |
| 2 | 764.4 | 725.7 |
| 3 | 630.6 | 624.6 |
| 4 | 779.3 | 802.7 |
| 5 | 640.3 | 693.0 |
| 6 | 636.8 | 678.6 |

#### 6.1.2.2 Maneuver Classification Performance

**Figure 18** shows the result of maneuver classification. From the results, we confirm precision and recall of *PUSH* are more than 87.1%. We also confirm the precision and recall of *PULL* are more than 74.8%. **Figures 19** and **20** show the maneuver classification performance of the left and right hand for each player.

**Table 4** Leave-one-person-out cross validation.

| ID | Threshold Setting $T^{PUSH}_\delta$ | Threshold Setting $T^{PULL}_\delta$ | F-measure *PUSH* | F-measure *PULL* | F-measure Both |
|---|---|---|---|---|---|
| 1 | 1.5 | 1.5 | 0.90 | 0.80 | 0.89 |
| 2 | 1.5 | 1.5 | 0.88 | 0.81 | 0.86 |
| 3 | 1.5 | 1.5 | 0.83 | 0.77 | 0.82 |
| 4 | 1.5 | 1.5 | 0.92 | 0.81 | 0.90 |
| 5 | 1.5 | 1.5 | 0.92 | 0.86 | 0.91 |
| 6 | 1.5 | 2.0 | 0.91 | 0.75 | 0.88 |
| All | - | - | 0.87 | 0.85 | 0.88 |

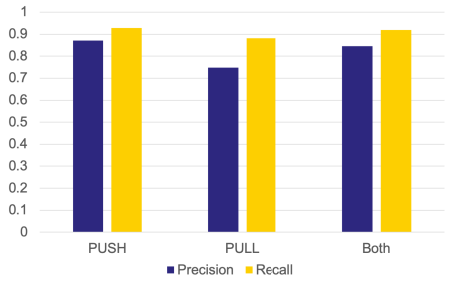


**Fig. 18** Average maneuver classification result.

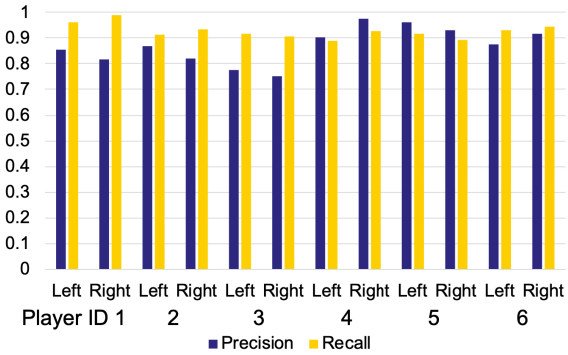


**Fig. 19** Classification performance of left and right hands for each player (*PUSH*).

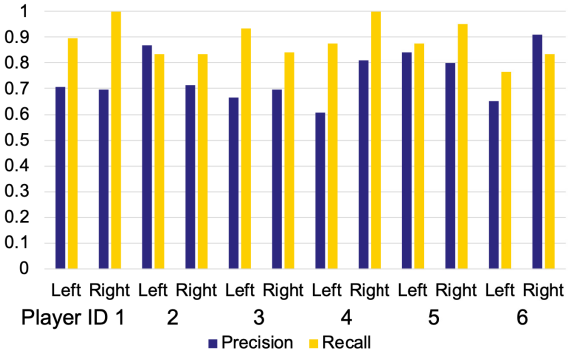


**Fig. 20** Classification performance of left and right hands for each player (*PULL*).

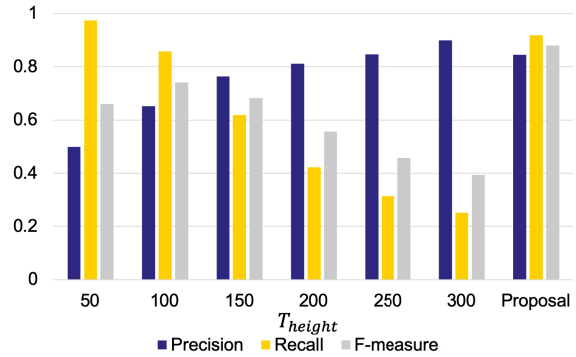


**Fig. 21** Performance when $T_{\text{height}}$ is fixed.

**Table 5** Turn dataset.

| Condition | Angle[degree] | # of *PIVOT* | # of *TURN* |
|---|---|---|---|
| Moving | 180 | 27 | 33 |
| | −180 | 25 | 39 |
| Stationary | 270 | 20 | 20 |
| | 180 | 20 | 20 |
| | 90 | 20 | 20 |
| | −90 | 20 | 20 |
| | −180 | 20 | 20 |
| | −270 | 20 | 20 |
| Total | | 172 | 192 |

From the results, we see that the *PUSH* classification performance is independent of hands in most cases. However, we also see the *PULL* classification performance is different between the left and right hands for players 2 and 6. Furthermore, as for player 4, recall of the left side is the lowest in all the players. Conversely, the precision of player 4's right side is the highest among the other players. This implies that the characteristics of the maneuver actions may differ slightly depending on hands and/or players. The results also mean our method can potentially assess the quality of maneuver. To improve the performance, in addition to the maximum speed, we may investigate the factors that can estimate the ability of individual players.

**Figure 21** shows the result when the threshold $T_{\text{height}}$ is fixed. When the threshold $T_{\text{height}}$ is low, the recall is high because it can detect small *PUSH* and *PULL*. However, the peaks and valleys due to noises are wrongly recognized as maneuvers, leading to low precision. On the other hand, when the threshold $T_{\text{height}}$ is high, precision becomes high while recall becomes low. This is because only maneuver actions with large movement are recognized. Our method achieves the highest F-measure, which means adjusting the threshold $T_{\text{height}}$ based on the speed works well.

### 6.2 Turn Classification

#### 6.2.1 Settings

In order to measure the turns while moving, we collected the data by repeating a turn after moving forward. We asked the player to make either a pivot turn or a spin turn in a specified direction (i.e., left or right). Also, in order to evaluate turns while stationary, we asked the player to make a turn with a specified angle from −270 to 270 [degree]. The leftward rotation is considered positive and the rightward rotation is considered negative. The summary of the collected data is as shown in **Table 5**. We observed 172 *PIVOT* and 192 *TURN*.

**Table 6** Turn classification result.

| | | Predicted Class *PIVOT* | Predicted Class *TURN* | Recall |
|---|---|---|---|---|
| True Class | *PIVOT* | 172 | 0 | 1 |
| | *TURN* | 1 | 191 | 0.9947 |
| | Precision | 0.9942 | 1 | |

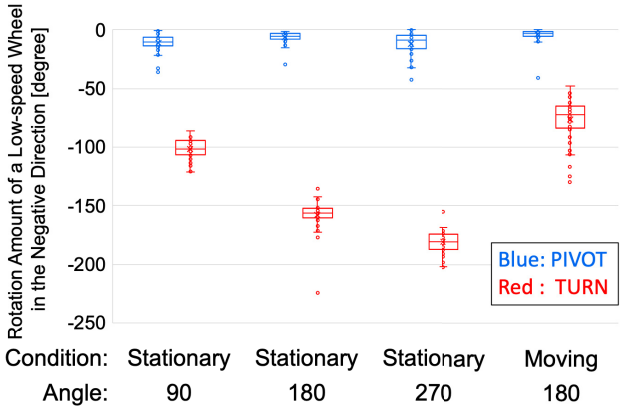


**Fig. 22** The amount of rotation of a low-speed wheel during a turn.

#### 6.2.2 Turn Classification Result

The results are shown in **Table 6**. The results show almost all the turns were correctly classified except only one *TURN* which is a spin turn during forward movement. To investigate the reason for the wrong classification, **Fig. 22** shows the amount of rotation of a low-speed wheel during a turn. This figure shows that it is difficult to change the moving direction of the wheel suddenly. As a result, the minimum amount of rotation of *TURN* during forward movement becomes closer to the maximum amount of rotation of *PIVOT* during stop. This leads to a wrong classification. This problem may be solved by considering the speed before a turn.

### 6.3 Use Cases on Data Analysis

#### 6.3.1 Difference between left and right hands

To see the difference between the left and right hands, we define the power of *PUSH* action in segment $s^i$ as the difference in the angular velocity (i.e., $\max_{t\in s^i}\omega(t) - \min_{t\in s^i}\omega(t)$). Then, we calculate the difference in the power between the left and the right wheels when *PUSH* is recognized for both of the wheels simultaneously. We assume the left and the right wheels are pushed simultaneously if both of the peaks at the end of the segments are detected within 0.5 seconds. **Figure 23** shows the distributions of the difference in power between the left and the right wheels. It is clear that 3 out of 6 players (players 1, 4, and 5) push the right wheel more strongly than the left wheel. This result implies that some players tend to rely on their dominant hands and to make turns in the same direction.

#### 6.3.2 Relationship between Maneuver Motions and Positions

We analyzed the relationship between the recognized maneuver actions and the positions. The players' positions are obtained from the video. For the analysis, the basketball court is divided into four areas by the foul lines and the center line as shown in **Fig. 24**. In this analysis, *PUSH* is categorized into two types depending on whether the angular velocity of the previous segment

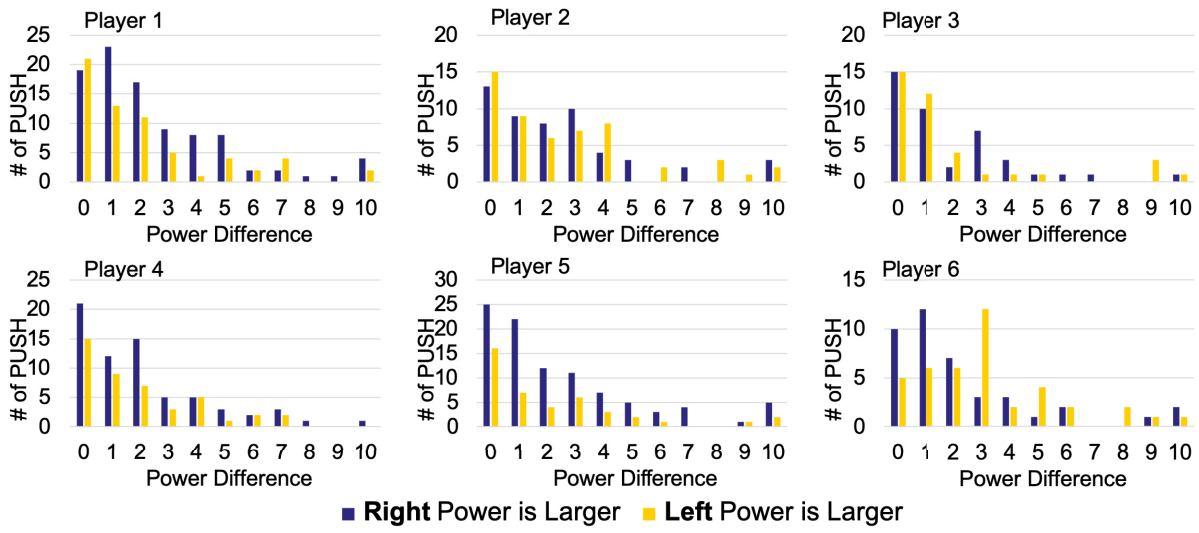


**Fig. 23** Power difference of left and right hands.

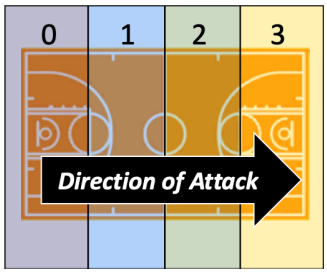


**Fig. 24** Basketball court divided into 4 areas.

**Table 7** Percentage of maneuver actions in each area [%].

| Area\Action | *PUSH* (Low) | *PUSH* (High) | *STOP* |
|---|---|---|---|
| 0 | 30.1 | 38.6 | 31.3 |
| 1 | 16.2 | 68.7 | 15.1 |
| 2 | 13.5 | 71.3 | 15.1 |
| 3 | 25.7 | 44.6 | 29.8 |

is above the threshold $\omega_{max}/4$ (high speed) or not (low speed).

**Table 7** shows the percentage of the maneuver types in each area. We see that high-speed *PUSH* exceeds 68.7% around the areas 1 and 2 which are the center of the areas. In particular, the percentage of *STOP* is extremely low in area 2 which is the first area of the opponent's court. This is because the players tend to accelerate rapidly for good movements when they are attacking. In addition, the result indicates that various maneuver types are mixed near the goals (i.e., the areas 0 and 3) because sophisticated movements are required to avoid or to interfere with opponents.

### 6.3.3 Sprint Comparison

In training, sprints are often practiced. **Figure 25** shows the speeds of two players over time in three trials of sprints at different distances. The left side is the speed of the left wheel and the right side is the speed of the right wheel. The x-axis is the number of *PUSH* actions. For example, the upper right figure shows player A reached 3.5 m/s at the fifth right hand *PUSH* for all the trials.

As seen from Fig. 25, in the short and long distance sprints, both players achieved almost the same speed with the same number of pushes. However, in the middle distance sprint shown in

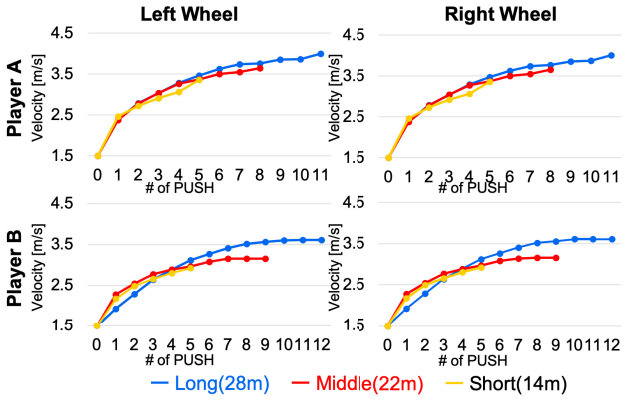


**Fig. 25** Speeds of 2 players over time in sprints at 3 different distances.

the red color, player B after the third *PUSH* shows a smaller increase in speed than yellow, which is long-distance sprint. This means that player A always achieved high performance in terms of speed regardless of distance.

## 7. Discussion

In this paper, we classify maneuver actions and turns for the purpose of assessing maneuvering quality. Our system allows confirming whether the players to confirm whether the players moved quickly and/or efficiently. It also helps them to improve their handling technique. For example, if a player tries to push a wheel with a strong force, that player can greatly accelerate all at once. At the same time, the force to grip the rim can become stronger, leading to larger deceleration of the wheel. By collecting practice data for sprints, players can understand how to efficiently reach the maximum speed without wasting force. Furthermore, we are planning to analyze the relation between the degree of disability and maneuver statistics measured by our system.

We note that, "better" actions often depend on situations. This means maneuver actions and turns recognized by our system may be not enough for analysis in games. To enable game analysis, we may integrate a video tracking system to use player positions that

reflect situations in a game. Such information about player positions enables us to consider what the best action is at the moment. For example, a player should conduct a pivot turn if an opponent is blocking the player's forward movement.

We assume our system will be used in training and practice games. In official games, the current rules for wheelchair basketball do not allow the use of sensors [16]. However, since data analysis in sports is becoming more common, the rules may change in the future.

## 8. Conclusion

In this paper, we propose two methods to detect and classify maneuver actions and turns of wheelchair basketball by using inertial sensors. Our design of the proposed method focuses on the specific movement of wheels. The evaluation results showed that our method achieves an F-measure of 88.1% for classification of maneuver actions. Also, our method achieves an F-measure of 99.7% for the classification of turns. Furthermore, we have shown usage cases for data analysis by using the classification results combined with other information such as player positions.

One topic for future work is applying in order to support technical improvement of maneuvering. For example, it is possible to achieve efficient training by quantifying the wheelchair maneuver actions through feedback to the players. In addition, visualization of changes in the maneuver actions over time may motivate the players. Furthermore, in cooperation with athletes and coaches, we are planning to develop a system to support data analysis in wheelchair basketball.

**Acknowledgments** This research is a part of the result of Sports Research Innovation Project (SRIP), FY2017 to FY2020 sponsored by Japan Sports Agency.

### References

[1] MARY ANN LIEBERT, INC.: How is big data impacting sports analytics? (online), available from ⟨https://www.eurekalert.org/pub_releases/2018-12/mali-hib122018.php⟩ (accessed 2019-02-01).
[2] Vanlandewijck, Y.C., Evaggelinou, C., Daly, D.J., Verellen, J., Van Houtte, S., Aspeslagh, V., Hendrickx, R., Piessens, T. and Zwakhoven, B.: The relationship between functional potential and field performance in elite female wheelchair basketball players, *Journal of Sports Sciences*, Vol.22, No.7, pp.668–675 (2004).
[3] De Lira, C., Vancini, R., Minozzo, F., Sousa, B., Dubas, J., Andrade, M., Steinberg, L. and Da Silva, A.: Relationship between aerobic and anaerobic parameters and functional classification in wheelchair basketball players, *Scandinavian Journal of Medicine & Science in Sports*, Vol.20, No.4, pp.638–643 (2010).
[4] van der Slikke, R., Berger, M. and Bregman, D.: Wheelchair mobility performance only supports the use of two classes in wheelchair basketball, *ISBS Proc. Archive*, Vol.35, No.1, p.254 (2017).
[5] Logan-Sprenger, H.M. and Mc Naughton, L.R.: Characterizing thermoregulatory demands of female wheelchair basketball players during competition, *Research in Sports Medicine*, pp.1–12 (2019).
[6] Hollander, K., Kluge, S., Glöer, F., Riepenhof, H., Zech, A. and Junge, A.: Epidemiology of injuries during the Wheelchair Basketball World Championships 2018: A prospective cohort study, *Scandinavian Journal of Medicine & Science in Sports*, Vol.30, No.1, pp.199–207 (2020).
[7] Van Der Slikke, R., De Witte, A., Berger, M., Bregman, D. and Veeger, D.: Wheelchair mobility performance enhancement by changing wheelchair properties: What is the effect of grip, seat height, and mass?, *International Journal of Sports Physiology and Performance*, Vol.13, No.8, pp.1050–1058 (online), DOI: 10.1123/ijspp.2017-0641 (2018).
[8] de Witte, A.M., Sjaarda, F.S., Helleman, J., Berger, M.A., Van Der Woude, L.H. and Hoozemans, M.J.: Sensitivity to change of the field-based Wheelchair Mobility Performance Test in wheelchair basketball, *Journal of Rehabilitation Medicine*, Vol.50, No.6, pp.556–562 (2018).
[9] Mason, B.S., Lemstra, M., van der Woude, L.H., Vegter, R. and Goosey-Tolfrey, V.L.: Influence of wheel configuration on wheelchair basketball performance: Wheel stiffness, tyre type and tyre orientation, *Medical Engineering & Physics*, Vol.37, No.4, pp.392–399 (2015).
[10] Wojke, N., Bewley, A. and Paulus, D.: Simple Online and Realtime Tracking with a Deep Association Metric, *2017 IEEE International Conference on Image Processing* (*ICIP*), pp.3645–3649, IEEE (online), DOI: 10.1109/ICIP.2017.8296962 (2017).
[11] Wojke, N. and Bewley, A.: Deep Cosine Metric Learning for Person Re-identification, *2018 IEEE Winter Conference on Applications of Computer Vision* (*WACV*), pp.748–756, IEEE (online), DOI: 10.1109/WACV.2018.00087 (2018).
[12] Redmon, J. and Farhadi, A.: YOLOv3: An Incremental Improvement, *ArXiv*, Vol.abs/1804.02767 (2018).
[13] Rabiner, L.R., McClellan, J.H. and Parks, T.W.: FIR digital filter design techniques using weighted Chebyshev approximation, *Proc. IEEE*, Vol.63, No.4, pp.595–610 (1975).
[14] The MathWorks, I.: Prominence (online), available from ⟨https://www.mathworks.com/help/signal/ug/prominence.html⟩ (accessed 2020-07-23).
[15] Rodríguez, N.E.N.: *Advanced Mechanics in Robotic Systems*, Springer Science & Business Media (2011).
[16] International Wheelchair Basketball Federation: 2018 OFFICIAL WHEELCHAIR BASKETBALL RULES (online), available from ⟨https://iwbf.org/wp-content/uploads/2019/03/2018_IWBF_rules-Ver-2_Final.pdf⟩ (accessed 2020-07-23).

**Ryosuke Hasegawa** received his M.E. degree in Information and Computer Science from Osaka University, Japan in 2019. He is Ph.D. student at Graduate School of Information Science and Technology, Osaka University, Japan. His current research interests include sensing and data analytics for sports. He is a member of Information Processing Society of Japan (IPSJ).

**Akira Uchiyama** received his M.E. and Ph.D. degrees in Information and Computer Science from the Osaka University in 2005 and 2008, respectively. He is an Assistant Professor at Graduate School of Information Science and Technology, Osaka University. He was a visiting scholar in the University of Illinois at Urbana-Champaign in 2008 and a research fellow of the Japan Society for the Promotion of Science from 2007 to 2009. His current research interests include mobile sensing and applications in pervasive and ubiquitous computing. He is a member of IEEE, ACM, IEICE and IPSJ.

**Takuya Magome** received his Ph.D. degree in Osaka University, United Graduate School of Child Department in 2014. He was an Endowed Chair Assistant Professor in Osaka University, Graduate School of Medicine, Department of Anatomy, Molecular Neuroscience (Sumitomo Dainippon Pharma Co., Ltd.) in 2014. He was an Assistant Professor in Osaka University, Graduate School of Medicine, Department of Anatomy, Neuroscience and Cell Biology from 2014 to 2015. He was Assistant Professor in Osaka University, Graduate School of Medicine, Department of Health and Sport Sciences, Sports Medicine from 2015 to 2018. He is Associate Professor in Otemon Gakuin University, Faculty of Sociology and Guest Associate Professor in Osaka University, Graduate School of Medicine, Department of Health and Sport Sciences, Sports Medicine from 2018. He is engaged in the Sports Research Innovation Project (SRIP) sponsored by Japan Sports Agency, and supports athletes in charge of "performance analysis".

**Juri Tatsumi** received her Master's degree of Sport Science, Osaka University of Sport and Health Sciences in 2015. She was a Specially Appointed Assistant Professor, Otemon Gakuin Univeristy, Institute of Liberal Arts in 2015. She was an Assistant Professor, Otemon Gakuin University, Institute of Liberal Arts from 2016 to 2018. She is Associate Professor in Otemon Gakuin University, Faculty of Sociology from 2019. She also is actively engaged in instructing artistic swimming.

**Teruo Higashino** received his B.S., M.S. and Ph.D. degrees in Information and Computer Sciences from Osaka University, Japan in 1979, 1981 and 1984, respectively. He joined the faculty of Osaka University in 1984. Since 2002, he has been a Professor in Graduate School of Information Science and Technology at Osaka University. His current research interests include design and analysis of distributed systems, communication protocol and mobile computing. He is a senior member of IEEE, a fellow of Information Processing Society of Japan (IPSJ), and a member of ACM and IEICE of Japan.